Mapping Forest Functional Type in a Forest-Shrubland Ecotone using SPOT Imagery and Predictive Habitat Distribution Modeling

TIMOTHY J. ASSAL[a, b*], PATRICK J. ANDERSON[a], and JASON SIBOLD[c],

[a]U.S. Geological Survey (USGS), Fort Collins Science Center, 2150 Centre Avenue, Fort Collins, CO 80526,
[b]Graduate Degree Program in Ecology, Colorado State University, 1401 Campus Delivery, Fort Collins, CO 80523, USA
[c]Department of Anthropology, Colorado State University, 1787 Campus Delivery, Fort Collins, CO 80523, USA

Corresponding author at: USGS, Fort Collins Science Center, Fort Collins, CO 80526, USA. Tel.: +1 970 226 9134.
E-mail address: assalt@usgs.gov (T.J. Assal).

Pre-print of published version.

Reference:

Assal, T., Anderson, P., Sibold, J., 2015. Mapping forest functional type in a forest-shrubland ecotone using SPOT imagery and predictive habitat distribution modelling. Remote Sens. Letters. 6, 755–764. doi:10.1080/2150704X.2015.1072289

http://www.tandfonline.com/doi/full/10.1080/2150704X.2015.1072289

Mapping Forest Functional Type in a Forest-Shrubland Ecotone using SPOT Imagery and Predictive Habitat Distribution Modeling

The availability of land cover data at local scales is an important component in forest management and monitoring efforts. Regional land cover data seldom provide detailed information needed to support local management needs. Here we present a transferable framework to model forest cover by major plant functional type using aerial photos, multi-date Système Pour l'Observation de la Terre (SPOT) imagery, and topographic variables. We developed probability of occurrence models for deciduous broad-leaved forest and needle-leaved evergreen forest using logistic regression in the southern portion of the Wyoming Basin Ecoregion. The model outputs were combined into a synthesis map depicting deciduous and coniferous forest cover type. We evaluated the models and synthesis map using a field validated, independent data source. Results showed strong relationships between forest cover and model variables and the synthesis map was accurate with an overall correct classification rate of 0.87 and Cohen's kappa value of 0.81. The results suggest our method adequately captures the functional type, size and distribution pattern of forest cover in a spatially heterogeneous landscape.

Keywords: Rocky Mountain forests, spatial heterogeneity, SPOT imagery, predictive habitat distribution models, logistic regression modeling, *Populus tremuloides*

1. Introduction

Land cover data provides the foundation for a wide variety of geographical analysis and science applications. There have been several national and regional land cover mapping

initiatives over the last two decades, most notably the National Land Cover Database (NLCD) (Jin et al. 2013), LANDFIRE (Rollins 2009), and ReGAP (Davidson et al. 2009). These products have provided tremendous utility in studies documenting land cover change (Radeloff et al. 2005), effects of climate change (Wylie et al. 2014), vegetation change (Bradley and Fleishman 2008) and conservation planning (Stoms 2000). However, in some heterogeneous ecosystems, they lack the spatial resolution needed to adequately characterize the extent and juxtaposition of land cover. In the Wyoming Basin ecoregion, small areas of forest are found within sagebrush shrubland at higher elevations which are difficult to adequately characterize using regional land cover data.

Plant functional types (PFTs) are groups of species that share similar structural, physiological and phenological traits (Barbour et al. 1999). PFTs provide a framework to consider how species utilize resource availability and respond to environmental change and management. At the stand scale, multispectral remote sensing can be used to delineate the relationship between vegetation structure and physiology of PFTs, linking biophysical properties to ecological theory (Ustin and Gamon 2010). Predictive habitat distribution modeling offers the potential to assess the current extent of species as well as effects of global climate change and other change agents. However, a challenge is to better link remote sensing data to underlying ecological relationships and describe the distribution of species along environmental gradients (Zimmermann et al. 2007). Incorporating remote sensing variables in the modeling process allows us to take full advantage of continuous gradients to delineate biophysical properties of vegetation such as leaf shape, structure, longevity and chlorophyll content (Jones and Vaughan 2010).

We explored the potential of fine-scale remotely sensed spectral data in predictive habitat distribution modeling of forest cover type across a forest-shrubland

ecotone. The two PFTs of interest in the study area are deciduous broad-leaved forest (referred to as deciduous forest) and montane needle-leaved evergreen forest (referred to as coniferous forest). We hypothesized that the delineation between forest functional type would be aided with the addition of multitemporal remote sensing predictors due to differences in phenology between deciduous and coniferous species (Bergen and Dronova 2007; Zimmermann et al. 2007). The major goal of the study was to develop an operational mapping framework using aerial photos coupled with fine-scale satellite imagery to efficiently model dominant forest cover. The specific objectives were to: 1) develop probability of occurrence models for deciduous and coniferous forest; and 2) to combine model outputs into a field-validated synthesis map depicting forest cover type.

2. Study Area

The study area, managed largely by the U.S. Bureau of Land Management, is located in the southern part of the Wyoming Basin ecoregion, spanning parts of southwestern Wyoming, northwestern Colorado, and northeastern Utah (Figure 1). Several prominent ridges form a transition zone between basins and mountainous areas (Knight 1994), where several species of trees exist at the xeric fringes of their respective ranges. Forests are dominated by either aspen (*Populus tremuloides*) or several coniferous species, namely subalpine fir (*Abies lasiocarpa*), Douglas-fir (*Pseudotsuga menziesii*), and lodgepole pine (*Pinus contorta*), that occur as relatively small patches on moist sites in a matrix of mountain sagebrush (*Artemisia tridendata* spp. *vaseyana*) or mixed-species shrublands. Scattered juniper (*Juniperus communis* var. *depressa*) and limber pine (*Pinus flexilis*) woodlands, distinct from the montane conifer forest, are found on rocky slopes at lower elevations and small patches of manzanita (*Arctostaphylos patula*) are found in the southern part of the study area. The area has a midlatitude steppe climate with a substantial portion of the annual precipitation occurring as snow.

Multiple state and federal agencies, along with the Wyoming Landscape Conservation Initiative (wlci.gov), have identified the region as a priority area for conservation given the important habitat it provides for many wildlife species. Drought-related mortality of aspen is a concern in western North America (Worrall et al. 2008), and lack of aspen regeneration due to high rates of herbivory is a concern locally. Active management seeks to address these concerns and locally accurate maps of forest cover type are critical to support conservation and monitoring efforts.

3. Methods

3.1 Explanatory Variables

We identified a contiguous area (1,088 km^2) greater than 2,300 m in elevation known to encompass the forest communities of the study area (Figure 1). We explored the relationship of topographic and multi-date remotely sensed variables to forest presence that have had utility in other SDMs (Turner et al. 2003; Zimmermann et al. 2007; Jarnevich et al. 2014; Engler et al. 2013). Topographic variables were derived from a 10 m National Elevation Data set and remotely sensed variables were derived from terrain corrected Level 1 T SPOT 5 HRG satellite imagery, acquired at no cost (USGS 2014) (Table 1). We obtained two cloud-free dates during leaf-on (07 September 2010) and leaf-off (19 October 2010) conditions from two SPOT scenes (KJ grid 555-267; 555-286). Each of the four images were geometrically registered to National Agriculture Imagery Program (NAIP) aerial photos using 20-25 ground control points with a root mean square error of less than 0.5 pixel. A top-of-atmosphere correction was applied to each image to account for differences in sensor and viewing angle (Wulder et al. 2006; Vogelmann et al. 2012; Sankey, Moffet, and Weber 2008).

Remotely sensed spectral bands and derived vegetation indices often exhibit high levels of collinearity (Engler et al. 2013). Multi-collinearity among all potential

explanatory variables was assessed prior to model calibration using the Pearson's correlation coefficient. Variables with a correlation coefficient greater than 0.8 or less than -0.8 were removed from consideration within the same model (Jarnevich et al. 2014). All of the analysis was conducted using the R statistical package (R Development Core Team 2013).

3.2 Sample Data

ReGAP land cover data was reclassified into eight land cover categories (including deciduous and coniferous forest), and we used a stratified random selection procedure to ensure an unbiased distribution of sample plots (10 m x 10 m, congruent with a SPOT pixel) across land cover types. Our objective was to capture fine-scale patterns in the study area, while minimizing the impact of spatial dependency between observations. We used a total of 545 plots, with a minimum distance of 250 m (25 pixels) between each plot, to develop presence and absence records. We interpreted recent aerial photographs (natural color and infrared NAIP) and classified each plot as deciduous forest, coniferous forest, or non-forest. Mixed forest is not found at broad scales in the study area, and it is difficult to reliably classify a 10 m NAIP plot as mixed forest. Absence records for deciduous forest included both non-forest and coniferous forest plots, whereas absence records for coniferous forest included non-forest and deciduous forest. We extracted the values of the 19 predictor variables (Table 1) at each sample location. The respective leaf-on and leaf-off periods for each band exhibited high collinearity. Leaf-on bands 1, 2, and 4 were also highly correlated along with leaf-on NDVI. We opted to use leaf-on bands over leaf-off, although leaf-off data was incorporated into ΔNDVI (Table 1). We retained band 1 over band 2 since information from band 2 is incorporated into the NDVI variable. This selection process resulted in

13 variables for consideration (Table 1), including longitude and latitude to account for spatial autocorrelation (Knapp et al. 2003; Hu and Lo 2007).

3.3 Data Analysis

Logistic regression is a widely used method to predict the probability of a dichotomous variable (i.e., presence, absence of a forest cover type) that has been used in species distribution modeling (SDM) (Engler et al. 2013; Jarnevich et al. 2014; Stohlgren et al. 2010) and other ecological studies (Turner et al. 2003; Wulder et al. 2006; Dubovyk et al. 2013). We used a multivariate generalized linear model (GLM, binomial distribution, logit link function) to create independent models of deciduous (DECID) and coniferous (CONIF) forest cover in the study area. We modeled each cover type independently to maximize information contained in the continuous gradient of biophysical characteristics of these systems. The full dataset (n = 545) was used for model calibration. To simplify the interpretation of the logistic model, we converted the regression coefficients into odds ratios, then calculated the percent change in odds (Wulder et al. 2006). This approach identifies the percent change in the probability of a pixel containing deciduous or coniferous forest relative to changes in independent variables.

We tested several models for each type of forest cover, using different combinations of predictor variables below the acceptable collinearity threshold. For each model a standard stepwise selection by Akaike's Information Criterion (AIC) was used to select the best subset of independent variables and we calculated variance inflation factors (VIF) to ensure all model variables had a value below 5 (Dubovyk et al. 2013). In logistic regression, spatial autocorrelation violates the assumption that observations are independent and can cause unreliable estimates of the model parameters (Hu and Lo 2007). We evaluated spatial autocorrelation using the Moran's I statistic on each model

using Pearson residuals which are comparable to residuals of linear regression models. The neighborhood structure of the spatial weights matrix was defined using inverse distance (Assal, Sibold, and Reich 2014).

The two selected models produced a continuous surface with values between zero and one corresponding to the probability of a pixel containing either deciduous or coniferous forest. We used an independent data set (n=321) representing coniferous, deciduous and non-forest observations to evaluate each model. The reference data set was compiled from observations of related studies that were visited in the field between 2010 and 2013. We randomly selected 100 presence and 100 absence points of the respective forest cover type for each model to calculate the receiver operator characteristic area under the curve (AUC). For each model, we selected a threshold where the sensitivity was equal to the specificity (Liu et al. 2005) (i.e. the number of false positives were equal to the number of false negatives) to convert each model output into a binary map of presence and absence.

3.4 Synthesis Map

The binary maps from the two models were combined into a synthesis map of deciduous and coniferous forest cover. If a pixel was predicted to contain both forest types, the values from each model above the presence threshold were linearly rescaled from 0 to 1. The cover type with the highest occurrence probability was then assigned to the pixel (Engler et al. 2013). Within each cover type, pixels were assigned to neighbors in all eight directions (‘queen’s move’) to identify contiguous forest patches. Patches of three pixels and greater were retained in order to minimize small, likely incorrect classified areas. We used the full, validation data set (n=321) to build a confusion matrix to calculate the overall classification accuracy and Cohen’s kappa coefficient on the synthesis map.

4. Results

Forest cover type was best predicted by a combination of topographic and spectral variables, and the two models included several common variables selected through the model fitting process (Table 2). The residuals of both models exhibited very weak or no spatial autocorrelation (DECID; Moran's I=0.005, p=0.052; CONIF; Moran's I=0.001, p=0.38). Aspen, the only deciduous forest type present, have a clonal growth form which produces clustered patches of deciduous forest in the study area. Both of the models had high accuracy with AUC values of 0.92 for DECID and 0.99 for CONIF. The percentage changes in the odds ratio for model variables are shown in Table 2. The DECID model indicated that the presence of deciduous forest is mainly associated with high values in the NIR band (band3.leaf-on), north facing slopes, and high values of ΔNDVI. Deciduous forest is more likely to be found in areas higher in elevation, particularly moderate elevations (classes 3 and 2). The model also indicated that deciduous forest was less likely associated with higher values in the green band (band1.leaf-on) and higher TPI values, found along ridge lines and hilltops. The CONIF model indicated presence of coniferous forest is mainly associated with high values in NDVI (NDVI.leaf-on), TPI and elevation and less likely associated with high values in the NIR band (band3.leaf-on) and areas that experience a higher HLI.

A comparison of the output maps, derived from the binary models, revealed high separation between the two models. Less than 1% of all pixels in the study area were predicted to contain both deciduous and coniferous forest. The comparison indicated satisfactory agreement with an overall classification accuracy of 87% (Table 3) and a Cohen's kappa coefficient (Cohen 1960) of 0.81. Our synthesis map identified 61.7 km^2 of forest (Figure 2). Deciduous forest accounts for 44% (27.2 km^2) of total forest cover, while the remaining 56% (34.5 km^2) is coniferous forest. There are over 7,000 patches

of deciduous forest compared to less than 2,400 coniferous forest patches, and the mean patch size is much smaller for deciduous (0.004 km^2) compared to coniferous forest (0.015 km^2).

5. Discussion

The spatial resolution (10 m) of the SPOT imagery appeared particularly appropriate for identifying the extent and pattern of forest cover in this highly heterogeneous ecosystem (Figure 3). The models performed well and had little overlap between forest functional types. Furthermore, we considered spatial autocorrelation in our framework which is often overlooked in SDMs. The inclusion of latitude and longitude in the model, as well as treating elevation as an indicator variable, accounted for spatial autocorrelation in the models. Consideration of plant physiology and species traits illuminates the ecological context of biophysical variables that were captured with leaf-on and leaf-off SPOT imagery. Due to differences in seasonal phenology, deciduous forests are more likely to be associated with areas that have a large ΔNDVI between leaf-on and leaf-off periods. Aspen leaves absorb more radiation (and reflect less) in the green region of the electromagnetic spectrum compared to sagebrush and grassland plants (Jones and Vaughan 2010). Therefore, deciduous forest is associated with lower values in the green band (band1.leaf-on) compared to shrubland and grasslands. Coniferous forests have higher NDVI values than grassland and shrubland, especially late in the growing season when the leaf-on image was acquired. Although deciduous forests have a higher NDVI than coniferous forests, NDVI was not as important in DECID, which also included ΔNDVI and the NIR band (band3.leaf-on). Coniferous forests do not reflect as much radiation as aspen forest, grassland, and sagebrush and, therefore, are more likely to be associated with lower values in the NIR (band3.leaf-on).

In our synthesis map, the non-forest class had the lowest producer's accuracy (the percentage of reference observations correctly mapped), due to Type 1 errors (i.e. false-positives) in the deciduous forest class (Table 3). The DECID model incorrectly classified some small areas of manzanita, non-forested riparian areas, narrow, linear bands of deciduous shrubs and one large herbaceous wetland. There is a trade-off between capturing small patches of deciduous forest and incorrectly classifying some small areas with similar spectral values to deciduous forest. In future work, our methodology could be improved with additional information that discriminates between herbaceous wetlands and deciduous forest. The deciduous forest class had the lowest user's accuracy (the percentage of map locations correctly identified) due to several type II errors (i.e. false-negatives). The higher rate of misclassification might be explained by the open canopy of aspen forests compared to closed, dense coniferous forest. Furthermore, some aspen stands observed in the field had a substantial amount of canopy dieback and tree mortality. Aspen forests with highly reduced leaf area at the time the satellite image was acquired have lower reflectance values and therefore tend to be mapped as non-forest. Although this can be a drawback, it highlights the value of our methodology to capture changes in aspen forest if fine-scale imagery is available over an appropriate time period. The CONIF model performed very strongly as needle-leaved species have a closed canopy that forms dense stands. A few exceptions include several conifer stands dominated by Douglas-fir that experienced high mortality in recent years due to infestation of the Douglas-fir beetle (*Dendroctonus pseudotsugae*).

6. Conclusions

We have presented a framework that incorporates aerial photos and satellite imagery to model dominant forest cover at local scales across a forest-shrubland ecotone. Our modeling process offers a powerful alternative to traditional image classification and

our synthesis map provides managers with an important tool to support conservation and monitoring efforts across management unit boundaries. Our study highlights the advantages of using physiologically relevant remote sensing products in predictive modeling and addresses an important research need (e.g. high-resolution remote sensing of aspen distribution, (Kulakowski, Kaye, and Kashian 2013)). We conclude that our approach is suitable to characterize the extent and juxtaposition of forest cover in a highly heterogeneous ecosystem. Furthermore, our framework utilizes open access aerial photos and satellite data. In this way it is transferable to highly heterogeneous ecosystems to develop critical baseline tree cover data that can be updated at regular intervals to monitor the effects of disturbance and long-term ecosystem dynamics.

Acknowledgements

This research was supported by the USGS Fort Collins Science Center and the Wyoming Landscape Conservation Initiative. Logistical support was provided by the Wyoming Game and Fish Department and Bureau of Land Management Rock Springs Field Office. We gratefully acknowledge Geneva Chong and two anonymous reviewers for their constructive comments. We thank Lucy Burris, Brian Cade, Alexandra Urza, Marie Dematatis, and Darlene Kilpatrick for discussion on research direction and/or assistance in collection of field data.

Any use of trade, firm, or product names is for descriptive purposes only and does not imply endorsement by the U.S. Government.

Table 1. Description of the explanatory variables considered in the analysis.

Variable	Description
Spectral variables	
Band1.leaf-on*	Green band (0.50 µm - 0.59 µm)
Band2.leaf-on	Red band (0.61 µm - 0.68 µm)
Band3.leaf-on*	Near infrared band (0.79 µm - 0.89 µm)
Band4.leaf-on*	Short wave infrared band (1.58 µm - 1.75 µm)
Normalized difference vegetation index (NDVI.leaf-on*)	NDVI = (B3 reflectance – B2 reflectance)/(B3 reflectance + B2 reflectance) (Rousse et al., 1974)
Band1.leaf-off	Green band (0.50 µm - 0.59 µm)
Band2.leaf-off	Red band (0.61 µm - 0.68 µm)
Band3.leaf-off	Near infrared band (0.79 µm - 0.89 µm)
Band4.leaf-off	Short wave infrared band (1.58 µm - 1.75 µm)
Normalized difference vegetation index (NDVI.leaf-off)	NDVI = (B3 reflectance – B2 reflectance)/(B3 reflectance + B2 reflectance) (Rousse et al., 1974)
ΔNDVI*	$\Delta NDVI = NDVI_{leaf\text{-}on} - NDVI_{leaf\text{-}off}$
Topographic variables	
Elevation*	Derived from National elevation data set
Slope*	Derived from National elevation data set
North exposure*	Cosine transformation of aspect
East exposure*	Sine transformation of aspect
Heat load index (HLI)*	Potential direct incident radiation (McCune & Keon, 2002; equation 3)
Topographic position index (TPI)*	A measure of slope position and landform type with respect to adjacent grid cells
Longitude*	Longitude at cell centroid
Latitude*	Latitude at cell centroid

Notes: Leaf-on variables were acquired from the 07 September 2010 SPOT image; leaf-off variables were acquired from the 19 October 2010 SPOT image. All variables have a spatial resolution of 10 m. The native resolution for band 4 is 20 m, but it was resampled to 10 m using a nearest neighbour transformation.

*Indicates variable was utilized in the modeling process.

Table 2. Predictor variables used in the logistic regression models.

Explanatory variable	DECID model		CONIF model	
	Coefficient	**Change in odds (%)**	**Coefficient**	**Change in odds (%)**
Spectral variables				
NDVI.leaf-on	-	-	1.9164*	580
ΔNDVI	0.3327*	39	-0.2914	-25
Band1.leaf-on	-4.261*	-99	-	-
Band3.leaf-on	3.068*	2050	-3.7485*	-98
Topographic variables				
TPI	-0.5016*	-39	0.8194*	127
HLI	-	-	-0.7466*	-53
North exposure	0.8654*	138	-0.6963	-50
Longitude	$-6.86e^{-05}$*	-	-	-
Latitude	$-1.24e^{-04}$*	-	-	-
Elevation**				
Class 1 (low)	-	-	-	-
Class 2 (low to moderate)	5.053*	15549	0.3221	38
Class 3 (moderate to high)	5.591*	26700	1.7885	498
Class 4 (High)	4.409*	-8119	3.5633*	3428

Notes: Estimates of the model parameters are listed for each model accordingly. **p-values* are significant at 0.05 or lower. **Elevation is treated as an indicator variable; therefore the percent change in odds for each class can only be compared to the reference elevation class (Class 1).

Table 3. Confusion matrix for the synthesis forest cover map.

Field data	Classified as:			Producer's accuracy (%)
	Non-forest	**Deciduous forest**	**Coniferous forest**	
Non-forest	**95**	24	3	78
Deciduous forest	6	**86**	5	89
Conifer forest	0	2	**100**	98
User's accuracy (%)	94.1	76.8	92.6	**87**

Note: bold values in the matrix diagonal highlight the correctly predicted samples.

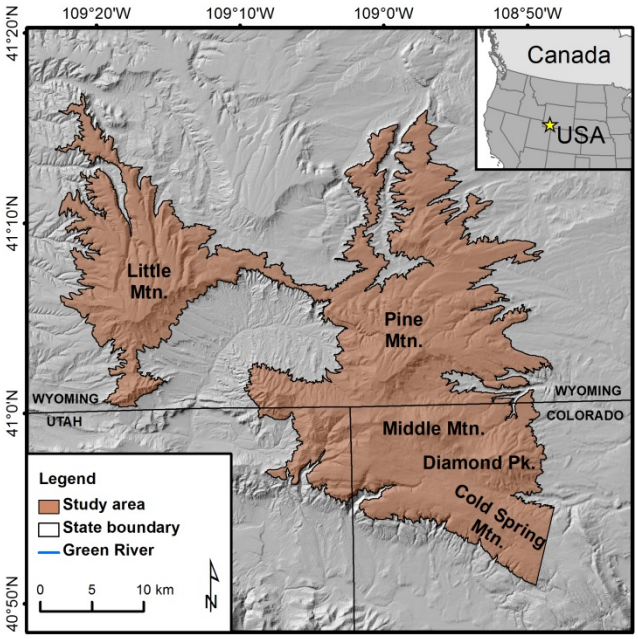

Figure 1. Location of study area. Note: approximately 50 km^2 of non-forest were omitted from the southeast corner of the study area due to the extent of the SPOT image.

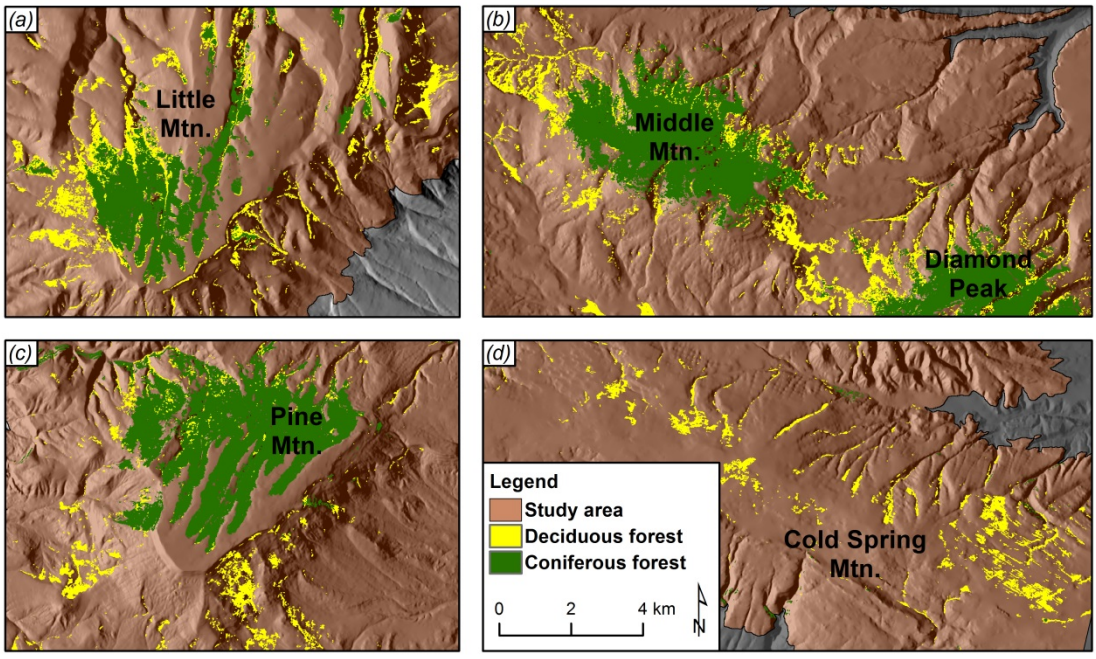

Figure 2. Results of the model outputs combined into the synthesis map: (*a*) Little Mountain, (*b*) Middle Mountain and portions of Diamond Peak, (*c*) Pine Mountain and (*d*) Cold Spring Mountain. Note: each map panel is displayed at the same scale.

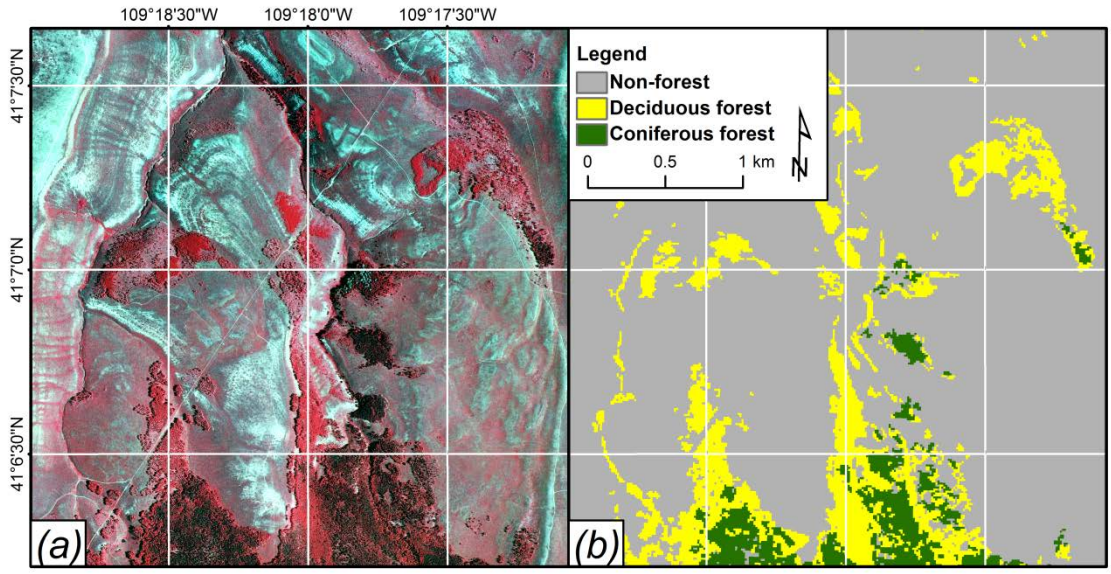

Figure 3. Comparison of forest type maps derived from each data source of a representative area of the landscape on Little Mountain: (*a*) 2009 color-infrared aerial photo (National Agriculture Imagery Program) where dark red/black hues indicate coniferous forest, red hues indicate deciduous forest, grey/light red/blue hues represent non-forest and (*b*) USGS synthesis map. Note: each map panel is displayed at the same scale and extent.

References

Assal, T.J., J. Sibold, and R. Reich. 2014. "Modeling a Historical Mountain Pine Beetle Outbreak Using Landsat MSS and Multiple Lines of Evidence." *Remote Sensing of Environment* 155 (December). Elsevier B.V.: 275–88. doi:10.1016/j.rse.2014.09.002.

Barbour, M.G., J.H. Burk, W.D. Pitts, F.S. Gilliam, and M.W. Schwartz. 1999. *Terrestrial Plant Ecology*. 3rd ed. New York, New York: Benjamin Cummings.

Bergen, K.M., and I. Dronova. 2007. "Observing Succession on Aspen-Dominated Landscapes Using a Remote Sensing-Ecosystem Approach." *Landscape Ecology* 22 (9): 1395–1410. doi:10.1007/s10980-007-9119-1.

Bradley, B.A., and E. Fleishman. 2008. "Relationships between Expanding Pinyon–juniper Cover and Topography in the Central Great Basin, Nevada." *Journal of Biogeography* 35 (5): 951–64. doi:10.1111/j.1365-2699.2007.01847.x.

Cohen, J. 1960. "A Coefficient of Agreement for Nominal Scales." *Educational and Psychological Measurement* 20: 37–46.

Davidson, A., J. Aycrigg, E. Grossmann, J. Kagan, S. Lennartz, S. McDonough, T. Miewald, et al. 2009. "Digital Land Cover Map for the Northwestern United States." Moscow, ID: Northwest Gap Analysis Project: USGS GAP Analysis Program.

Dubovyk, O., G. Menz, C. Conrad, E. Kan, M. Machwitz, and A. Khamzina. 2013. "Spatio-Temporal Analyses of Cropland Degradation in the Irrigated Lowlands of Uzbekistan Using Remote-Sensing and Logistic Regression Modeling." *Environmental Monitoring and Assessment* 185 (6): 4775–90. doi:10.1007/s10661-012-2904-6.

Engler, R., L.T. Waser, N.E. Zimmermann, M. Schaub, S. Berdos, C. Ginzler and A. Psomas. 2013. "Combining Ensemble Modeling and Remote Sensing for Mapping Individual Tree Species at High Spatial Resolution." *Forest Ecology and Management* 310: 64–73.

Hu, Z., and C. Lo. 2007. "Modeling Urban Growth in Atlanta Using Logistic Regression." *Computers, Environment and Urban Systems* 31 (6): 667–88. doi:10.1016/j.compenvurbsys.2006.11.001.

Jarnevich, C.S., W.E. Esaias, P.L.A. Ma, J.T. Morisette, J.E. Nickeson, T.J. Stohlgren, T.R. Holcombe, J.M. Nightingale, R.E. Wolfe, and B. Tan. 2014. "Regional Distribution Models with Lack of Proximate Predictors: Africanized Honeybees Expanding North." Edited by Mark Robertson. *Diversity and Distributions* 20 (2): 193–201. doi:10.1111/ddi.12143.

Jin, S., L. Yang, P. Danielson, C. Homer, J. Fry, and G. Xian. 2013. "A Comprehensive Change Detection Method for Updating the National Land Cover Database to circa 2011." *Remote Sensing of Environment* 132: 159–75.

Jones, H.G., and R.H. Vaughan. 2010. *Remote Sensing of Vegetation: Principles, Techniques, and Applications*. Oxford, UK: Oxford University Press.

Knapp, R.A., K.R. Matthews, H.K. Preisler, and R. Jellison. 2003. "Developing Probabilistic Models to Predict Amphibian Site Occupancy in a Patchy Landscape." *Ecological Applications* 13 (4): 1069–82.

Knight, D.H. 1994. *Mountains and Plains: The Ecology of Wyoming Landscapes*. New Haven, Connecticut: Yale University.

Kulakowski, Dominik, Margot W. Kaye, and Daniel M. Kashian. 2013. "Long-Term Aspen Cover Change in the Western US." *Forest Ecology and Management* 299 (July). Elsevier B.V.: 52–59. doi:10.1016/j.foreco.2013.01.004.

Liu, C., P.M. Berry, T.P. Dawson, and R.G. Pearson. 2005. "Selecting Thresholds of Occurrence in the Prediction of Species Distributions." *Ecography* 28 (December 2004): 385–93.

McCune, B., and D. Keon. 2002. "Equations for Potential Annual Direct Incident Radiation and Heat Load." *Journal of Vegetation Science* 13 (4): 603–6.

R Development Core Team. 2013. "R: A Language and Environment for Statistical Computing." Vienna, Austria: R Foundation for Statistical Computing. http://www.r-project.org/.

Radeloff, V.C., R.B. Hammer, S.I. Stewart, J.S. Fried, S.S. Holcomb, and J.F. McKeefry. 2005. "The Wildland-Urban Interface in the United States." *Ecological Applications* 15 (3): 799–805.

Rollins, M.G. 2009. "LANDFIRE: A Nationally Consistent Vegetation, Wildland Fire, and Fuel Assessment." *International Journal of Wildland Fire* 18 (3): 235–49.

Rousse, J.W., R.H. Hass, J.A. Schell, D.W. Deering, and J.C. Harlan. 1974. *Monitoring the Vernal Advancement of Retrogradation of Natural Vegetation*. *Type III, Final Report*. Greenbelt, Maryland.

Sankey, Temuulen Tsagaan, Corey Moffet, and Keith Weber. 2008. "Postfire Recovery of Sagebrush Communities: Assessment Using Spot-5 and Very Large-Scale Aerial Imagery." *Rangeland Ecology & Management* 61 (6): 598–604. doi:10.2111/08-079.1.

Stohlgren, T.J., P. Ma, S. Kumar, M. Rocca, J.T. Morisette, C.S. Jarnevich, and N. Benson. 2010. "Ensemble Habitat Mapping of Invasive Plant Species." *Risk Analysis* 30 (2): 224–35. doi:10.1111/j.1539-6924.2009.01343.x.

Stoms, D.M. 2000. "GAP Management Status and Regional Indicators of Threats to Biodiversity." *Landscape Ecology* 15: 21–33.

Turner, M.G., W.H. Romme, R.A. Reed, and G.A. Tuskan. 2003. “Post-Fire Aspen Seedling Recruitment across the Yellowstone (USA) Landscape.” *Landscape Ecology* 18: 127–40.

USGS. 2014. “EarthExplorer Archive.” http://edcsns17.cr.usgs.gov/NewEarthExplorer/.

Ustin, S.L., and J.A. Gamon. 2010. “Remote Sensing of Plant Functional Types.” *New Phytologist* 186: 795–816. doi:10.1111/j.1469-8137.2010.03284.x.

Vogelmann, J.E., G. Xian, C. Homer, and B. Tolk. 2012. “Monitoring Gradual Ecosystem Change Using Landsat Time Series Analyses: Case Studies in Selected Forest and Rangeland Ecosystems.” *Remote Sensing of Environment* 122 (July). Elsevier B.V.: 92–105. doi:10.1016/j.rse.2011.06.027.

Worrall, J.J., L. Egeland, T. Eager, R.A. Mask, E.W. Johnson, P.A. Kemp, and W.D. Shepperd. 2008. “Rapid Mortality of Populus Tremuloides in Southwestern Colorado, USA.” *Forest Ecology and Management* 255 (3-4): 686–96. doi:10.1016/j.foreco.2007.09.071.

Wulder, M.A., J.C. White, B.J. Bentz, M.F. Alvarez, and N.C. Coops. 2006. “Estimating the Probability of Mountain Pine Beetle Red-Attack Damage.” *Remote Sensing of Environment* 101: 150–66.

Wylie, B., M. Rigge, B. Brisco, K. Murnaghan, J. Rover, and J. Long. 2014. “Effects of Disturbance and Climate Change on Ecosystem Performance in the Yukon River Basin Boreal Forest.” *Remote Sensing* 6 (10): 9145–69. doi:10.3390/rs6109145.

Zimmermann, N.E., T.C. Edwards, G.G. Moisen, T.S. Frescino, and J.A. Blackard. 2007. “Remote Sensing-Based Predictors Improve Distribution Models of Rare, Early Successional and Broadleaf Tree Species in Utah.” *The Journal of Applied Ecology* 44 (5): 1057–67. doi:10.1111/j.1365-2664.2007.01348.x.